J. Appl. Comput. Mech., 11(4) (2025) 961-974
DOI: 10.22055/jacm.2024.47305.4692

ISSN: 2383-4536
jacm.scu.ac.ir

Shahid Chamran
University of Ahvaz

Journal of
Applied and Computational Mechanics

Research Paper

Relation of Muscles Coordination to the Major Degrees of Freedom in Three Upper Limb Motions

Morteza Farrokhnia[1], Seyyed Arash Haghpanah[1], Esmaeal Ghavanloo[1], Mohammad Taghi Karimi[2]

[1] School of Mechanical Engineering, Shiraz University, Shiraz 71963-16548, Iran

[2] Rehabilitation Sciences Research Center, Shiraz University of Medical Sciences, Shiraz, Iran

Received July 01 2024; Revised November 01 2024; Accepted for publication December 12 2024.
Corresponding author: S.A. Haghpanah (haghpanah@shirazu.ac.ir)

Abstract. The development of musculoskeletal models aims to facilitate the evaluation of muscle function and coordination during daily activities. These models are validated using surface electromyography (EMG) data to ensure accurate representation of neuromuscular activation patterns. After validation, dominant muscles in each phase of motion are identified through non-negative matrix factorization (NNMF) and inverse kinematics (IK) approaches. The study considers three specific motions: flexion/extension, abduction/adduction, and shrugging. Using the NNMF approach, four synergies are identified for the flexion and abduction motions, while two synergies are identified for the shrugging motion. Given the high degrees of freedom (DOF) in the shoulder complex, the IK approach is employed to detect the major DOF involved in each movement. Therefore, the dominant muscles associated with the major DOF are determined based on the literature. This study investigates how the central nervous system generates muscle activation patterns to coordinate complex joint movements, a challenge in motor control. The results show high conformity between muscle coordination and the dominant muscles identified by the IK and NNMF approaches, confirming the validity of using NNMF to describe muscle coordination strategies. Based on the findings, a simplified musculoskeletal model (SMM) is proposed for predicting joint angles in the upper limbs of prostheses and robotic applications. This model incorporates identified synergy modules and key joint DOF for the three basic motions, reflecting the underlying principles of motor control for efficient movement execution.

Keywords: Electromyography data; Motor control; Muscle synergy; Musculoskeletal model.

1. Introduction

Knowledge about the structure and function of human musculoskeletal system is necessary to investigate the muscles and kinematic coordination. In addition, measuring all muscle forces using experimental methods is impossible due to the deep muscles. Hence, the musculoskeletal systems have the significant role to simulate the motions and calculate the muscle forces [1, 2].

In existing human musculoskeletal systems, various approaches have been proposed to characterize the mechanics of the limbs [3, 4]. In the first approach, the gliding plane motion of the scapula on thorax is considered by one or two fixed scapula points constrained to an ellipsoid surface [5, 6]. This approach has been proven to show an unrealistic motion. The second approach is to determine the orientation of the scapula and the clavicle as a function of humeral motion by regressive equations known as the scapulohumeral rhythm. The second approach will also fail to display the scapula motion independent of the humerus [7, 8]. In the third approach for musculoskeletal modelling of shoulder, the effects of large thoracoscapular muscles were ignored; while these muscles have important role in force generation [9]. To overcome this point, Odle et al. [10] considered the large thoracoscapular muscles, but maintained the coupled scapular kinematics to the humeral rotation that caused large forces during different phases of the movement. After that, Seth et al. [11] developed a shoulder musculoskeletal model which includes large thoracoscapular muscles and the uncoupled movement of the scapula with respect to the humerus. Their model was validated via the muscle activations obtained from the experiment and modelling.

Since it is impossible to measure muscle forces directly through experiments, optimization approaches are employed to estimate these forces. By optimizing load sharing, joint moments are distributed among muscles to compute muscle forces in the lower limbs [12]. Also, the inverse dynamic approach has been proposed to provide joint moments to compute joints forces in musculoskeletal models [13, 14]. The optimization technique estimates the muscles forces by applying the cost function including muscles activation subject to net joints moments as the constraints due to the existence of more muscles than the equilibrium equations [15, 16]. In addition, the muscle co-contraction for upper extremity by applying the optimization of load sharing [17] or by measuring the electromyography (EMG) data [18, 19] in some previous studies. Sarshari et al. [20] presented a novel EMG assisted load sharing method to estimate the GH joint reaction force for verifying the musculoskeletal model. The load sharing optimization underestimated antagonist muscle forces. therefore, they applied the EMG data into the musculoskeletal model. Although, the measured EMG data is able to estimate muscle co-contractions more directly however, The EMG-driven model suffers from inaccuracies due to signal crosstalk among multiple muscles, which affects the accuracy of muscle activation estimates. To address this, a combination of measured EMG data and computed muscle control (CMC) is applied to enhance the accuracy of simulating muscle coordination [21]. CMC is an optimization-based approach used to estimate the necessary muscle activations during actual motion. It achieves this by summing muscle activations and applying a set of equality constraints to distribute loads among muscles, thereby producing observed movements while minimizing differences between the simulated and actual motions.

Understanding how the central nervous system (CNS) controls the complexity of the musculoskeletal system is challenging [22, 23], as it requires the coordination of multiple muscles for various tasks [24]. For example, in flexion motion, some muscles must be coordinated to stabilize the scapula, while others must be coordinated to move the humerus [25]. To distinguish the dominant muscles in each phase of motion and the activation time of each synergy, mathematical methods are applied to the EMG data. Different algorithms such as nonnegative matrix factorization (NNMF), principal component analysis (PCA) and independent component analysis (ICA) are used to find a subset of vectors that characterize the EMG signals. The advantage of NNMF over other synergy extraction methods lies in its non-negativity constraint, which aligns more closely with the physiological realities of muscle function in biological systems. In contrast, PCA and ICA have disadvantages related to data averaging, orthogonality, and statistical independence [26]. The subspace of four to six synergies has been proposed to explain muscle activation in humans for walking, and upper-extremity tasks [21]. Previous studies have mostly focused on lower limb synergies, with some exploring trunk and upper extremity coordination during paraplegic gait [27].

Despite numerous studies on synergy analysis of the lower limbs, the analysis of upper limbs, including muscle coordination and their relation to the joints' degrees of freedom (DOF), remains a gap in the research. The purpose of this study is to identify the relationships between muscle group activations and the major DOF involved in each phase of motion. This understanding will be valuable for designing rehabilitation devices, particularly for paralyzed muscles.

In this paper, a shoulder musculoskeletal model with seven joints and eleven DOF is verified with the EMG data extracted from three healthy subjects. To predict muscle activation of the musculoskeletal model, two simulation platforms, namely inverse kinematic (IK) and computed muscle control (CMC), are used. The IK approach calculates joint angles based on the kinematics of markers attached to the upper body segments. In contrast, the CMC approach, an optimization-based method, is used to compute the muscle activations needed to produce the observed movements from these joint angles. All simulations are performed using OpenSim and MATLAB. Muscle activations of the musculoskeletal modelling are compared to track the measured and processed EMG data. The experiments are done during three basic movements flexion/extension, abduction/adduction and shrugging. By analyzing these three basic movements, the muscles synergies in complex motions which are composed of these three basic movements can be identified.

In the experiments, the EMG data of eight muscles are measured and processed to obtain the muscles activations. The musculoskeletal model which is developed by Seth et al. is used due to considering large thoracoscapular muscles and the independent motion of the scapula with respect to the humerus.

To verify the musculoskeletal model, the root mean square error (RMSE) and the mean absolute error (MAE) between the modeled and experimental muscle activations are calculated. After model verification, the muscles synergies of the flexion, abduction and the shrugging motion considering twenty-one muscles activations are extracted. Identifying synergies in different motions helps us understand how muscles cooperate during various movements and identify synergist muscles that can compensate when one muscle is weakened. The number of synergies is different in each motion. The dominant muscles in each synergy and the activation time of each muscle are extracted from activation coefficient and synergy versus time diagram obtained from the NNMF method.

In addition to the NNMF method to extract dominant muscles in different phases of motion, the major DOF and the phase diagram of each joint DOF that compose the full range of motion are extracted by applying the IK method. The muscles contributing to the major DOF are identified for all three motions based on the literature review. Then, the dominant muscles obtained from the NNMF are compared with the muscles contributing to the major DOF. The main contributions of the current study are as follows:

- To validate the dominant muscles recognized by the IK and the NNMF approaches.
- To detect the relation of synergies activation to the phases of motion.
- To propose the simplified musculoskeletal model (SMM) with synergy modules and the major DOF.

The proposed SMM, incorporating synergy modules and major DOF, will enhance the design of rehabilitation protocols and assistive devices. By targeting key joint actions and muscle synergy groups, it reduces the dimensionality of the problem and improves our understanding of movement mechanics.

2. Material and Methods

2.1. Shoulder musculoskeletal model

In this study, we use a shoulder musculoskeletal model proposed by Seth et al. [9]. The model consists of the thorax, scapula, clavicle and humerus as shown in Fig. 1(a), and includes seven joints, eleven DOF and thirty-three muscles bundles. The most challenging joint in upper limb is scapulothoracic joint which is defined by the translation and rotation of the scapula on simulated ellipsoid-shaped surface of the thorax. The ellipsoid-shaped mobilizer is similar to a ball-and-socket joint; however, the key difference is that the body remains perpendicular to the surface of the ellipsoid, preventing pure rotational motion, as shown in Fig. 1(c). Consequently, the scapula contacts the thorax, which is approximated by an ellipsoid surface. The scapulothoracic joint reference frame is located at the centroid of the scapula and it can be parameterized by four coordinates including scapula abduction/adduction, elevation/depression, upward rotation, and internal rotation (winging) as indicated in Fig. 1(b). In addition, the sternoclavicular joint is usually modeled by a universal joint to produce protraction-retraction and elevation-depression motion of the clavicle. Also, the GH joint is modeled as a gimbal joint to produce shoulder elevation, plane elevation and axial rotation of the humerus motion based on the International Society of Biomechanics (ISB) standard [28]. Two other DOF are elbow flexion/extension and pronation/supination of radioulnar joint.

2.2. Computational methods

2.2.1. Scaling process

The scaling process is crucial for personalizing the musculoskeletal model for subject-specific applications. This process aims to adjust a generic musculoskeletal model to better match the physical characteristics of a specific subject. The dimensions of the model segments are adjusted based on the ratio of the subject's measured segment lengths to the original model segment lengths.

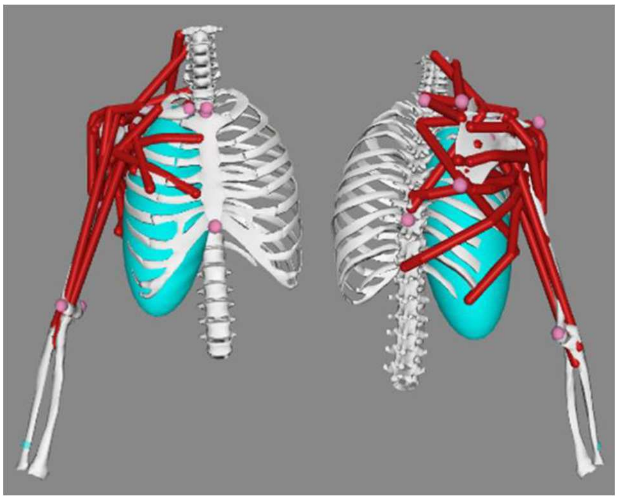

(a)

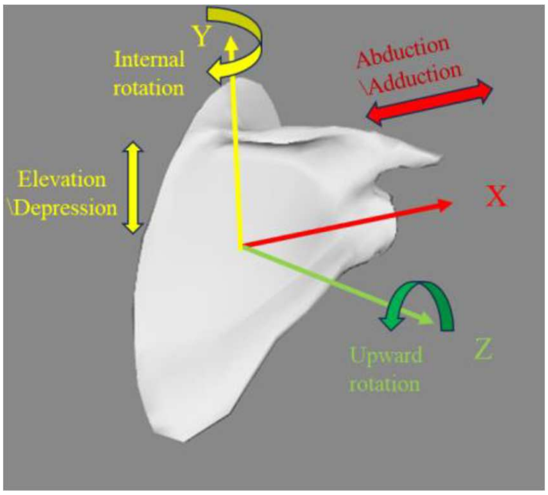

(b)

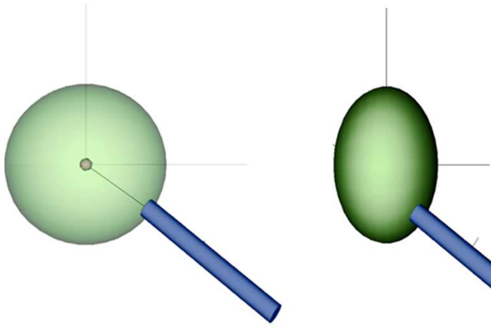

(c)

Fig. 1. Musculoskeletal model; (a) Shoulder complex muscles, (b) scapulae DOF, and (c) Ball-and-socket and ellipsoid mobilizers [29].

2.2.2. Inverse kinematic (IK)

The IK method computes the generalized coordinates by optimizing the differences between the position of markers in the experiment and modelling. The weighted least square will be solved to find the solution to minimize the marker and coordinate values as follows:

$$\min_{q}\left[\sum_{i\in markers} w_i \left\| x_i^{\exp} - x_i(q)\right\|^2 + \sum_{j\in coordinates} \omega_j (q_j^{\exp} - q_j)^2\right] \tag{1}$$

where q is the vector of generalized coordinate which will be solved by $x_i^{\exp}$ as the experimental position of marker "i", $x_i(q)$ as the position of the model marker and $\ddot{\vec{q}}^{des}$ is the experimental value for coordinate "*j*". In the following, the obtained generalized coordinates will be used in CMC approach.

2.2.3. Computed Muscle Control (CMC)

CMC is an optimization-based method used to estimate muscle activations required to replicate observed movements in musculoskeletal models. It involves calculating the muscle forces needed to achieve the desired joint moments while minimizing the difference between the simulated motion and the actual recorded motion. CMC differs from traditional inverse dynamics approaches, which calculate joint moments based on external forces and motion data without directly estimating individual muscle forces. Unlike inverse dynamics, CMC accounts for muscle redundancy and optimizes muscle coordination to generate the desired joint moments, thus providing a more physiologically realistic estimate of muscle forces. CMC is a tracking-based inverse controller to estimate muscle activations for the desired motions. The first step of this method is to calculate the desired acceleration of joint angle ($\ddot{\vec{q}}^{des}$) as follows [30]:

$$\ddot{\vec{q}}^{des} = \ddot{\vec{q}}^{\exp} + k_v(\dot{\vec{q}}^{\exp} - \dot{\vec{q}}) + k_p(\vec{q}^{\exp} - \vec{q}) \tag{2}$$

where $\vec{q}$ and $\dot{\vec{q}}$ are the generalized coordinates and velocities respectively, $\vec{q}_{\exp}$, $\ddot{\vec{q}}_{\exp}$ and $\dot{\vec{q}}_{\exp}$ are respectively denoted the experimental positions, velocities and accelerations corresponding to the generalized coordinates of the model. In addition, the gains for position and velocity errors are denoted as k_p and k_v, respectively. The required joint torques (τ) needed to achieve the desired accelerations are computed using inverse dynamics from the dynamic model:

$$\tau_j = M\ddot{q}_{des} + C\dot{q} + G \tag{3}$$

where *M* is the mass (inertia) matrix, *C* accounts for Coriolis and centrifugal forces, and *G* accounts for gravitational forces. Additionally, the muscle activations (a_i) are modeled to generate joint torques. The torque produced by muscles is given by the following equation:

$$\tau_j = \sum_{i=1}^{n_a} r_{ij} a_i F_{\max,i} f(l) f(v) \tag{4}$$

where r_{ij} is the moment arm of muscle i at joint j, n_a is the number of muscles, $F_{\max,i}$ is the maximum isometric force of muscle i, and $f(l)$ and $f(v)$ are functions representing muscle length and velocity effects, respectively.

To compute the desired muscle activation for producing the desired acceleration, a static optimization method is utilized. For this optimization, the following cost function, J, is defined and minimized [31]:

$$J = \sum_{i=1}^{n_a} a_i^{\,2} + \sum_{j=1}^{n_q} w_j\Big(\tau_j - \sum_{i=1}^{n_a} r_{ij} a_i F_{\max,i} f(l) f(v)\Big)^2 \qquad 0 < a_i < 1 \tag{5}$$

in which n_q is the number of DOF and w_j is a penalty weight coefficient. The CMC is repeated in each step time until the final time of the simulation based on the muscle activation constraint $0 < a_i < 1$.

2.2.4. Extraction of muscle synergy

Muscle synergy can be defined by using various approaches by either time-dependent or time-independent parameters. In this paper, the time-independent formulation is used to derive synergy space for the three specified motions and the NNMF method is utilized to extract muscles synergies.

Generally, m neural commands are necessary to control m muscles. However, these m commands can be reduced to a low-dimensional subspace by using the NNMF approach. In this approach, the data matrix $F^{m\times t}$ (t is the number of data points), which consists the EMG's data, decomposes as a product of muscle synergy matrix $W^{m\times n}$ and activation matrix $\mathbf{C}^{n\times t}$ (n is the number of synergies) and $E^{m\times t}$ is the reconstruction error matrix. Although the decomposition provides an exact reconstruction data, the matrix $F^{m\times t}$ can be rewritten as [32]:

$$F_r^{m\times t} = W^{m\times n}\mathbf{C}^{n\times t} + E^{m\times t} \tag{6}$$

The NNMF algorithm is implemented in Python and solves an optimization problem that minimizes the reconstruction error (usually the norm of the difference between F and $W \times C$), subject to the non-negativity constraints on W and C.

To compute the minimum number of muscle synergies required to reconstruct muscle activation adequately, variance accounted for (*VAF*) is defined as the follows [33]:

$$VAF = \left(1 - \frac{\sum_{i=1}^{m}\sum_{j=1}^{t} E_{ij}^2}{\sum_{i=1}^{m}\sum_{j=1}^{t} F_{ij}^2}\right) \times 100 \tag{7}$$

If the value of *VAF* is larger than 90%, the number of synergies is adequate. The 90% threshold for *VAF* is commonly adopted as it strikes a balance between statistical significance, model simplicity, and the interpretability of muscle synergy identification. According to previous studies, *VAF* index for each muscle should exceed 90% when comparing computed muscle activations to the product of the muscle synergy and activation coefficient matrices [27].

2.3. Experimental setup

In this study, the cyclic shoulder flexion/extension in the sagittal plane, the abduction/adduction in the frontal plane and the shrugging motion of the right-hand side of the shoulder complex were performed by three healthy volunteers. These motions were chosen to extract the synergies of basic upper limb movements. Participants were equipped with bipolar surface electrodes, with a sampling frequency of 1000 Hz, as shown in Fig. 2. All experiments were done at the Motion Analysis Lab under supervision of the Research Ethics Committee, School of Rehabilitation Sciences, Shiraz University of Medical Sciences. All the subjects involved in the experiments gave informed consent to the work. To evaluate muscle cooperation, it is sufficient to consider three healthy participants with no neurological disorders, based on previous studies. However, a limitation of this work is that subjects must perform upper limb motions while electromyography and kinematic markers are attached to their skin. Eight surface muscles considered in these experiments are anterior (AD), posterior deltoids (PD), superior trapezius (TS), serratus anterior (SA), pectoralis major sternal head (PM-Stern), teres major (T-major), biceps (Bic) and triceps (Tri). These eight muscles were selected because they are superficial and play a dominant role in various motions, according to a previous study [11]. All motions were performed for three times. In addition, the trajectories of twelve bony landmarks were measured using the eight cameras (ProReflex, QualisysR Ltd., Sweden) at 100 Hz sampling frequency to track the markers fixed to the skin. A low-pass filter is applied to the motion capture data to smooth the signals, with a cutoff frequency set at 4 Hz to reduce noise. Gap filling is used to create a continuous dataset by addressing any missing data, and spline interpolation is employed to estimate these missing data points. The bony landmarks are incisura jugularis (IJ), processus xiphoideus (PX), 7th cervical vertebra (C7), 8th thoracic vertebra (T8), sternoclavicular (SC), acromioclavicular (AC), angulus acromialis (AA), medial epicondyle (EM), lateral epicondyle (EL), radial styloid (RS), and ulnar styloid (US).

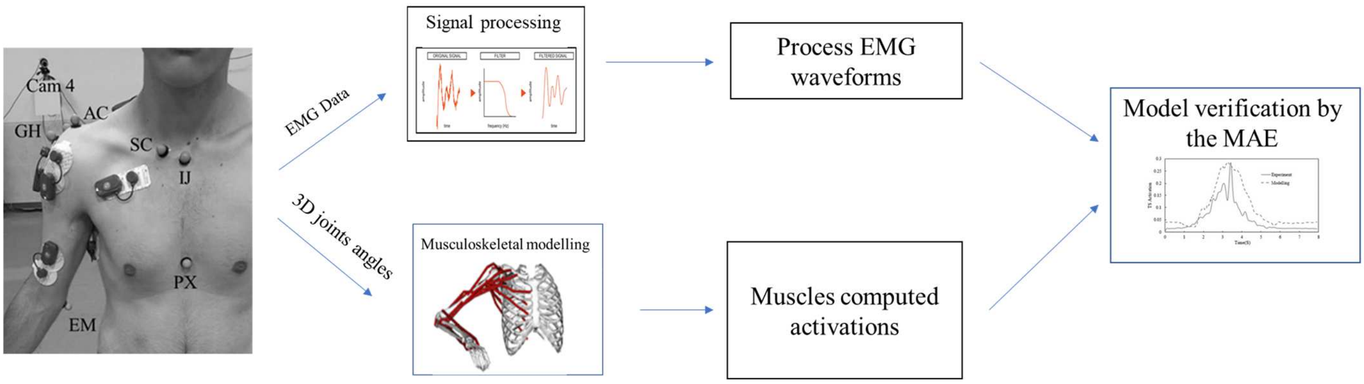

Fig. 2. Kinematic and electromyography measurement devices.

All original EMG signals were preprocessed to extract effective EMG signals. A Butterworth high-pass filter (fourth order, cutoff frequency of 100 Hz) was applied to the raw EMG signals for filtering and rectification. Subsequently, a Butterworth low-pass filter (fourth order, cutoff frequency of 4 Hz) was used to obtain the EMG envelope. Each EMG channel was then normalized to the maximum observed value. To ensure the reliability of the measurements, both kinematic and electromyography devices were calibrated. Participants of similar ages were selected, and each performed the motions in different cycles over 30 seconds. To validate the experiments, the placement of the electromyography devices was cleaned and determined according to the Surface Electromyography for the Non-Invasive Assessment of Muscles (SENIAM) guidelines on the muscle belly. The distance between electrodes was standardized to minimize noise.

3. Model Verification

In the first step, the IK approach is applied to eleven DOF musculoskeletal model for obtaining the joint angles. To calculate the muscles activations, the CMC approach is used according to joints angles, angular velocities and accelerations. Then, the activations of twenty-one muscles are extracted from the output of the musculoskeletal model. Eight muscles which are similar to the experimentally measured EMG data are chosen. To verify the musculoskeletal model, the activations of AD, PD, TS and SA muscles obtained from the model for the flexion/extension motion and those measured experimentally are shown in Fig. 3. The comparison of the results reveals that muscle activation patterns computed from the musculoskeletal model are acceptable agreements to the experimental patterns. The RMSE and the MAE between the measured EMG data and the model muscle activations for all motions are presented in Table 1. The comparison of these results demonstrates that the muscle activation patterns computed from the musculoskeletal model show acceptable agreement with the experimental patterns [34, 35].

After verifying the model, we are now looking into extracting the muscles synergies for the flexion/extension, the abduction/adduction and the shrugging motions. In this way, twenty-one muscles are considered in synergy extraction. These muscles are deep and measuring the EMG data of these muscles is impossible. Therefore, the verified musculoskeletal model and the NNMF approach are used to detect the dominant muscles.

4. Results

4.1. Synergy extraction

The NNMF approach is applied to extract synergies of upper limb motions. To extract the minimum number of synergies VAF with the threshold of 90% for each muscle are introduced to explain muscle activations of twenty-one muscles [27].

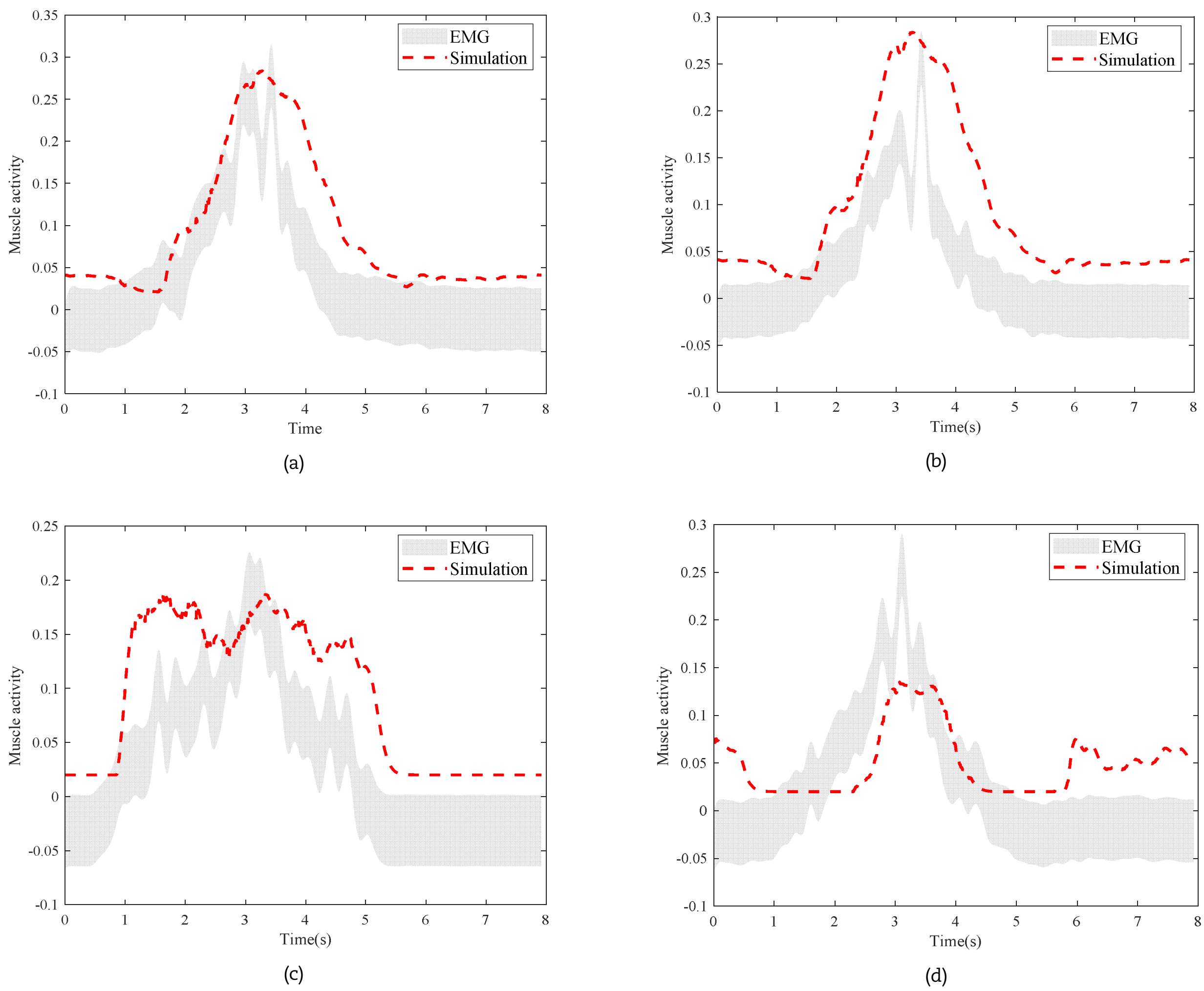

Fig. 3. Comparison of the experimental and simulated muscles activations for (a) SA, (b) TS, (c) AD, and (d) PD muscles.

Table 1. The RMSE and MAE between the measured EMG data and model muscle activation.

Tasks	AD		PD		TS		SA		PM-Clavi		T-Major		Biceps		Tri	
	RMSE	MAE	RMSE	MAE	RMSE	MAE	RMSE	MAE	RMSE	MAE	RMSE	MAE	RMSE	MAE	RMSE	MAE
Flx/Ex	0.1	0.04	0.08	0.02	0.10	0.05	0.08	0.04	0.09	0.04	0.1	0.05	0.15	0.07	0.11	0.05
abd/add	0.12	0.09	0.12	0.06	0.17	0.10	0.07	0.03	0.08	0.01	0.08	0.02	0.09	0.03	0.06	0.03
Shru	0.07	0.01	0.08	0.01	0.14	0.09	0.09	0.04	0.11	0.06	0.06	0.01	0.15	0.08	0.12	0.06

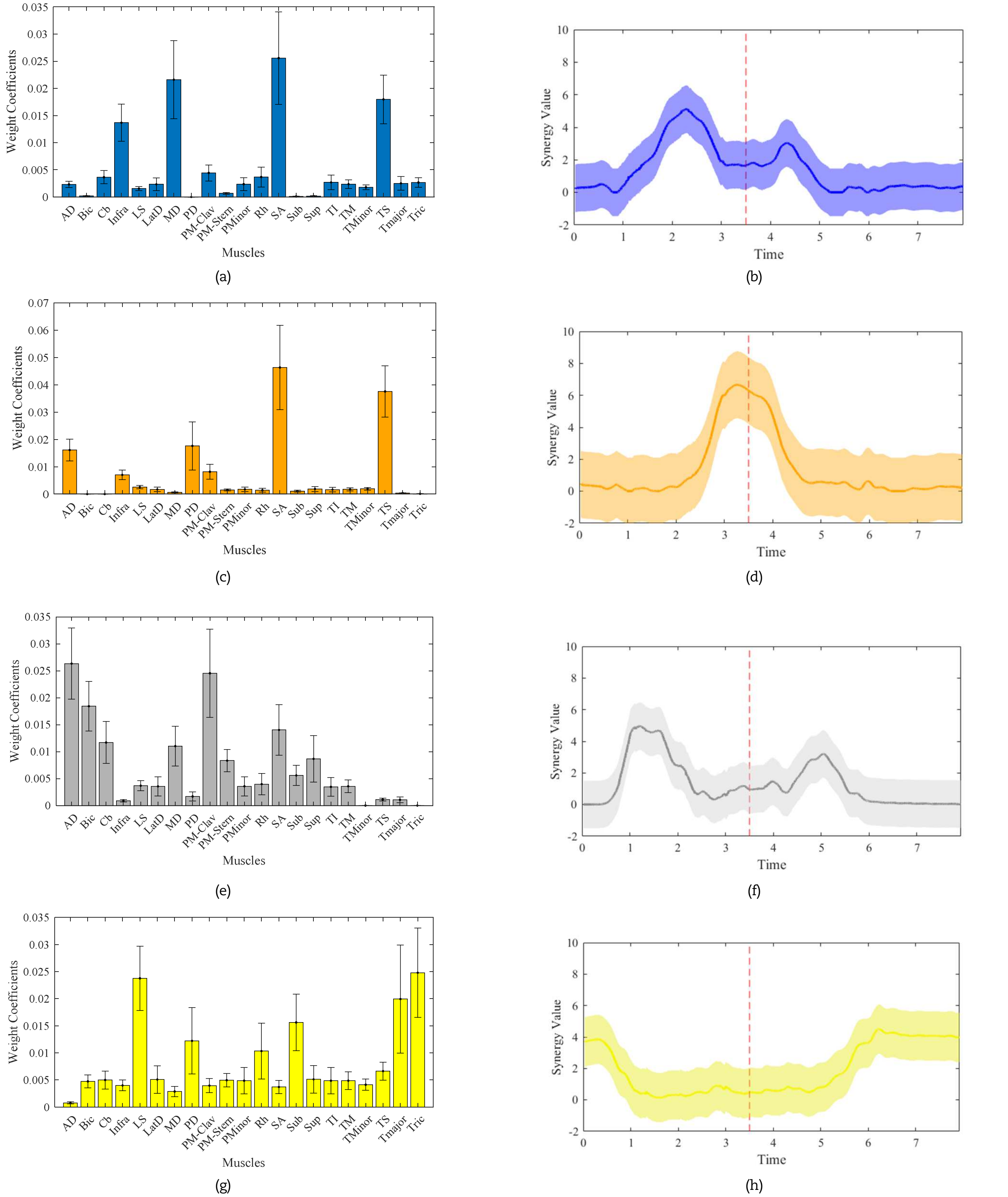

Fig. 4. Spatiotemporal patterns of four muscle synergies in flexion/extension motion; (a), (c), (e) and (g) show the temporal pattern, and (b), (d), (f), and (h) show the spatial patterns of the four muscle synergies 1-4.

Table 2. The Shapiro-Wilk test in each synergy for flexion motion.

	W Statistic		W Statistic
Synergy 1	0.78	Synergy 3	0.87
Synergy 2	0.74	Synergy 4	0.84

4.1.1. *Flexion/extension motion*

After applying the NNMF approach, The VAF index for each muscle is performed to be more than 90 percent for each muscle in three subjects. The standard deviation (SD) index was used to investigate the variation in muscle synergies obtained from the three subjects. The extracted synergies and their activation coefficients, along with their SD values, are presented in Fig. 4. The cyclic flexion motion is performed in two phases, the first phase of the motion is 0-180 degree (0-3.5s) and the second phase is 180-0 degree (3.5-7.9s). Figure 4 shows that the synergy value 3 of the flexion motion will be activated mostly in the initial two thirds of the first phase of cyclic motion because of the peak value zone in the synergy diagram in the interval time of 1 to 2 seconds and synergy value 4 will decrease in the first phase of motion and increase in the second phase of motion. This shows that the dominant muscles activate in the extension mode (180 to 0 degrees). It is shown in Fig. 4, that synergy 2 will be activated at the end of the first phase and the beginning of the second phase and a peak value is existed when direction change of the motion is happened.

Variations in muscle synergies between subjects are depicted in the shaded areas of the synergy patterns. These shaded areas represent the standard error of the mean across subjects, while the error bars indicate the standard deviation of the mean. The distribution of activation coefficients for different muscles in each synergy was assessed using the Shapiro-Wilk test, as shown in Table 2. The p-values for all synergies exceed 0.05, indicating a normal distribution of the activation coefficients.

4.1.2. *Abduction/Adduction motion*

For the abduction/adduction motion, results obtained from the NNMF approach reveal that, to achieve a threshold level of 90% VAF, four muscle synergies are necessary to explain muscle activations of twenty-one muscles. The extracted synergies and their activation coefficients are shown in Fig. 5. The cyclic abduction motion is performed in two phases, the first phase of the motion is 0-180 degree (0-7.2s) and the second phase is 180-0 degree (7.2-10.9s).

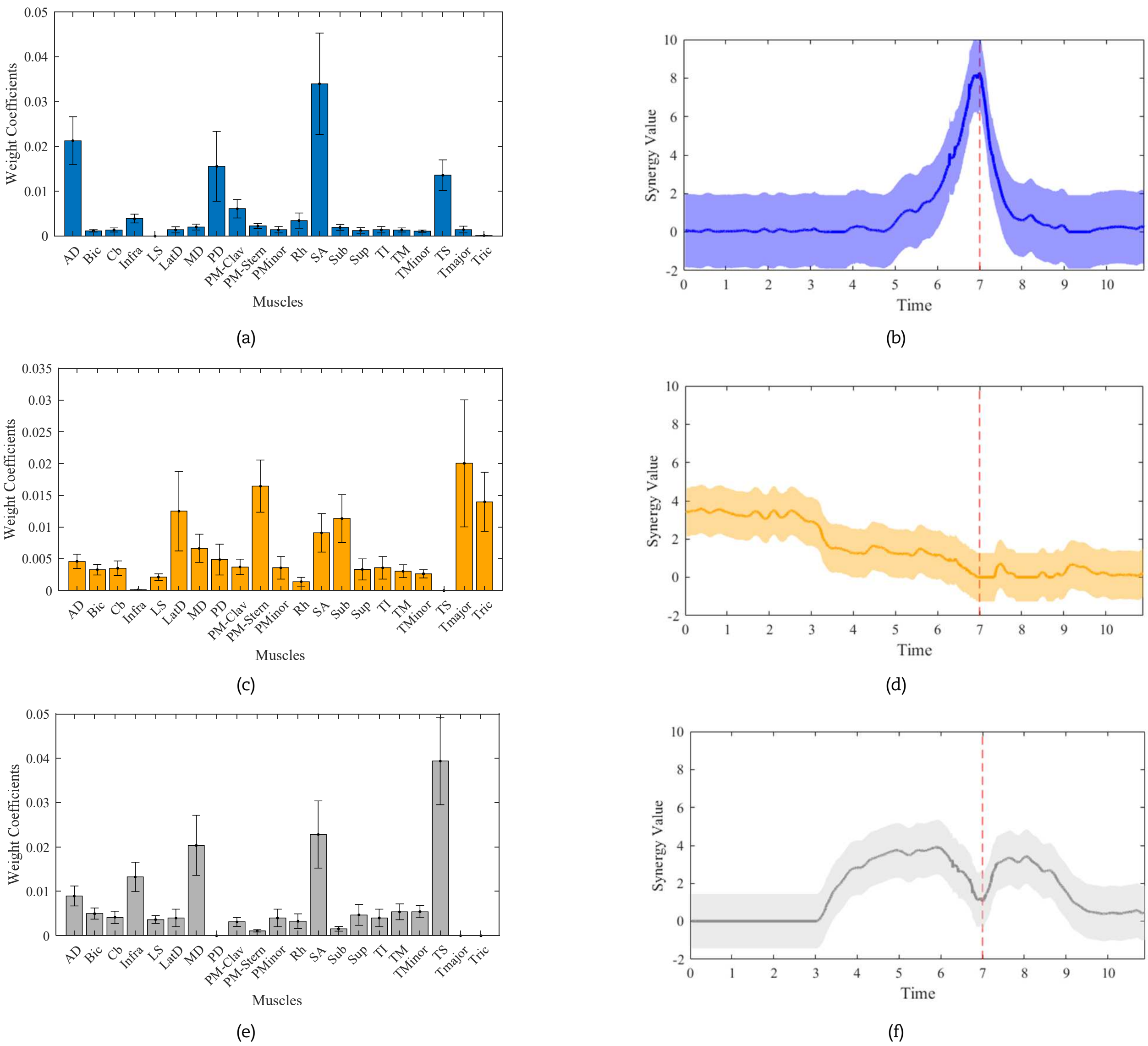

Fig. 5. Spatiotemporal patterns of four muscle synergies in abduction motion; (a), (c), (e), and (g) show the temporal pattern, and (b), (d), (f), and (h) show the spatial patterns of the four muscle synergies 1-4.

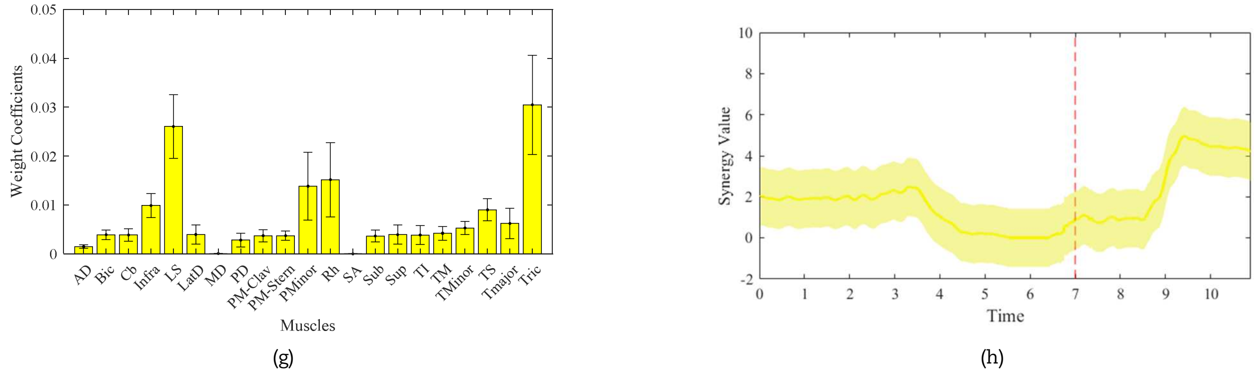

Fig. 5. Continued.

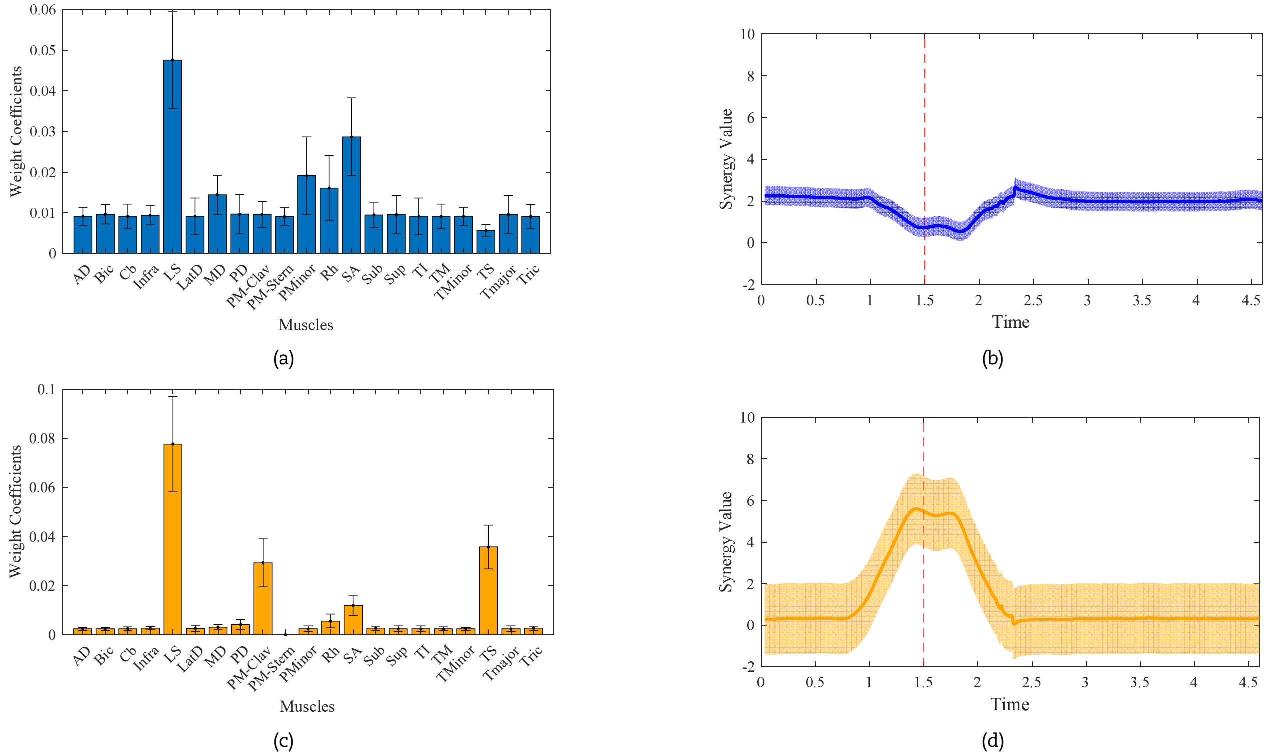

Fig. 6. Spatiotemporal patterns of two muscle synergies in shrugging motion; (a) and (c) show the temporal pattern, and (b) and (d) show the spatial patterns of the two muscle synergies 1-2.

Based on the results of the Fig. 5, Synergy 3 shows the increase at the end of the first phase of motion (0-180) and the beginning of second phase of motion (180-0) that is related to the initial two thirds of the first phase of cyclic motion and the initial one thirds of the second phase of motion. In the other hand, the value of the Synergy 4 will decrease in the first phase and will increase in the second phase of the motion that is shown to be activated in the second phase of the motion. It is shown in Fig. 5, that synergy 1 will be activated at the end of the first phase and the beginning of the second phase and a peak value is existed when direction change of the motion is happened. The results of the Shapiro-Wilk test for the abduction motion, indicating the distribution of muscle activation coefficients in each synergy, are presented in Table 3. The p-values for all synergies exceed 0.05, demonstrating a normal distribution of the activation coefficients.

4.1.3. *Shrugging motion*

For the shrugging motion, results obtained from the NNMF approach demonstrate that, to achieve a threshold level of 90% VAF, two muscle synergies are necessary to explain muscle activations of twenty-one muscles. The extracted synergies and their activation coefficients are plotted in Fig. 6. The cyclic shrugging motion is performed in two phases, the first phase of the motion is 0-80 degree (0-1.5s) and the second phase is 80-0 degree (1.5-4.6s). Based on the results of Fig. 6, two synergies act against each other and the time of motion direction change, synergy 1 decrease and synergy 2 increase. The Shapiro-Wilk test was conducted to investigate the distribution of data for the shrugging motion, as shown in Table 4. The p-values for each synergy are greater than 0.05, indicating a normal distribution.

Table 3. The Shapiro-Wilk test in each synergy for abduction motion.

	W Statistic		W Statistic
Synergy 1	0.75	Synergy 3	0.78
Synergy 2	0.84	Synergy 4	0.82

Table 4. The Shapiro-Wilk test in each synergy for shrugging motion.

	W Statistic		W Statistic
Synergy 1	0.82	Synergy 2	0.74

Table 5. The significant results of independent t-test for synergies in different motions.

	Synergy patterns	t-static		Synergy patterns	t-static		Synergy patterns	t-static
Flex- Abd	W1-W3	1.23	Flex-Shr	W2-W2	0.12	Abd-Shr	W1-W2	0.53
	W2-W1	0.63		W4-W1	1.15		W2-W1	1.27
	W3-W3	0.97					W4-W1	0.97
	W4-W2	1.46						
	W4-W4	0.25						

Table 6. The number of synergies and the dominant muscles in each synergy.

	Flex	Abd	Sh
Number of Synergies	4	4	2
Dominant muscles in each synergy			
W1	SA MD Infra Ts	SA TS PD AD	LS Pminor SA
W2	SA TS PD AD	PM LatD T-Major Sub	LS TS
W3	AD PM-Clav Bic Cb	MD TS SA Infra	
W4	Tric T-major PD Sub	LS Rh Pminor Tmajor Tric	

Given the normality of the synergy coefficients (p-value > 0.05), an independent t-test was conducted to investigate significant differences across different motions. Table 5 presents the significant results of the independent t-test among the three motions. There is no significant difference in the specified synergies between any two motions, as the p-values for these synergies are greater than 0.05.

The dominant muscles which cooperate in each synergy of the motion are shown in the muscles weight coefficient diagram. Dominant muscles are identified based on their relative maximum activation compared to other muscles. This means that some muscles act as primary movers in each phase of motion, exhibiting higher activation coefficient values than others. The standard deviation of synergies is calculated to indicate the variation in activation coefficients and synergy values during the motions among the three subjects. The number of synergies and the dominant muscles in each synergy for the VAF more than 90 percent is shown in Table 6. In the following the other method to distinguish the dominant muscles of the motion is presented. Then, the results of two approaches are compared.

4.2. Studying on the joints DOF

In this section, the kinematic data of eleven upper limb joints DOF are measured. The DOF of GH includes shoulder elevation, shoulder plane elevation and shoulder axial rotation. The SC joint includes scapula abduction, scapula elevation, scapula upward rotation and scapula winging. The DOF of SC joint are clavicular protraction and clavicular elevation. The DOF of radioulnar joint is pronation/supination and another DOF is elbow flexion. Due to the complexity of the shoulder complex and the high number of upper limbs DOF, finding the minimum major DOF which composes the full range of motion is desirable. Each joint DOF versus time is computed by using the IK method and plotted in Fig. 7 for three motions. By studying the summation of the joint angles, the major DOF, which composes approximately the full range of motion, is chosen in each motion.

Based on the results, it can be seen that the flexion motion occurs due to the interaction between GH and SC joints. The majority of the flexion motion is composed of the shoulder elevation of the GH joint and the scapula upward rotation of the SC joint. Furthermore, in flexion motion, the shoulder elevation of the GH joint with contributing the scapula upward rotation of the SC joint will extend the humerus up to 160 degrees according to the round dot of the Fig. 8(a). It is concluded that the scapula upward rotation is the most effective motion of SC joint to complete the flexion motion in the phase of 90 to 180 degrees of the shoulder complex. Figure 8(a) shows the kinematic data of all upper limb joints DOF in dash line. The joints DOF which are effective in flexion motion are shoulder elevation, scapula upward rotation, scapula winging, clavicle protraction, shoulder plane elevation and pronation/supination of the radioulnar joint. The summation of the major DOF is shown in solid line.

Similar to the flexion motion, the abduction motion is the result of the interaction between the GH and the SC joints. The majority of the abduction motion is composed of the shoulder elevation of the GH joint and the scapula upward rotation of the SC joint. The joints DOF which are effective in abduction motion are shoulder elevation, scapula upward rotation, clavicle protraction, shoulder plane elevation and pronation/supination of the radioulnar joint. Figure 8(b) shows the motion of shoulder complex due to the summation of five major joints DOF in the abduction motion Also, the summation of the two major DOF shoulder elevation and scapula upward rotation is shown in the round dot in Fig. 8(b).

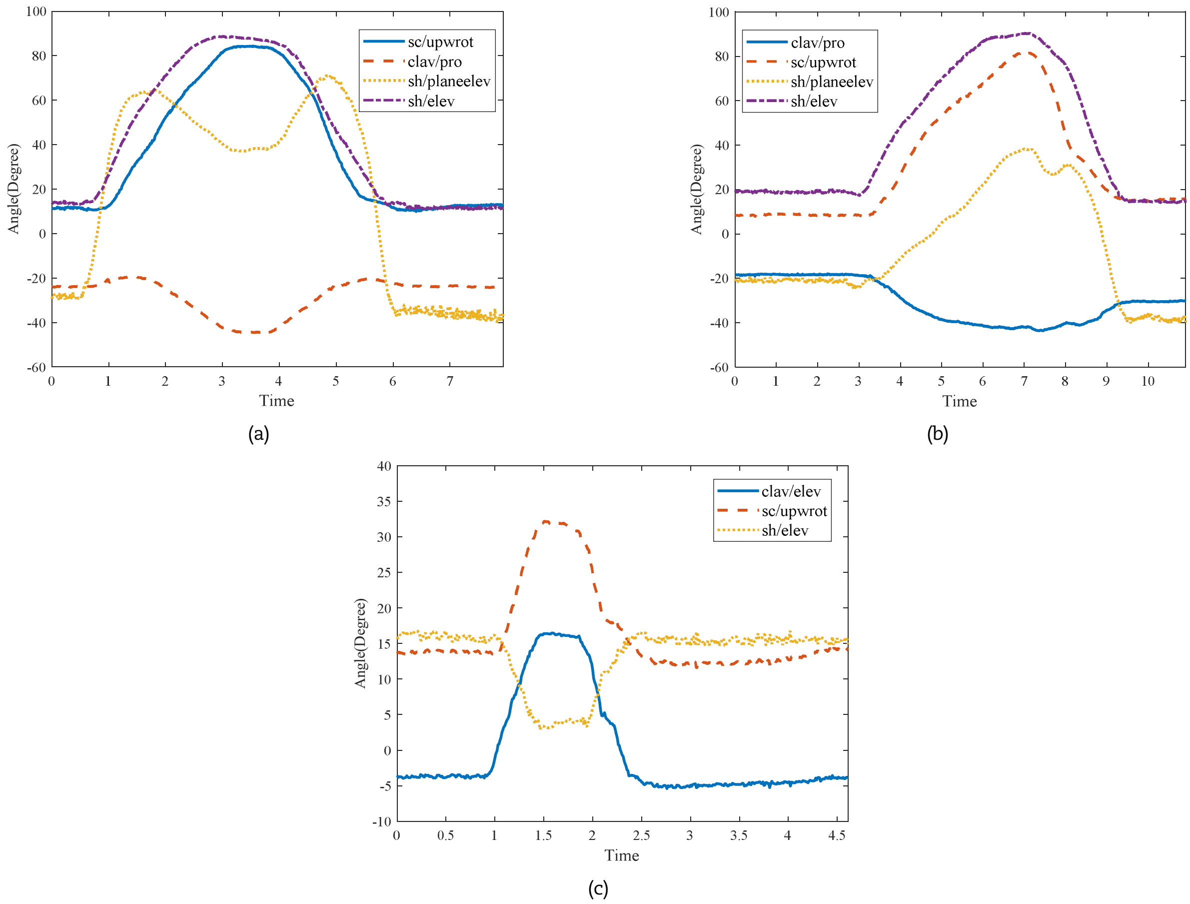

Fig. 7. Joints DOF versus time in (a) flexion, (b) abduction, and (c) shrugging motions.

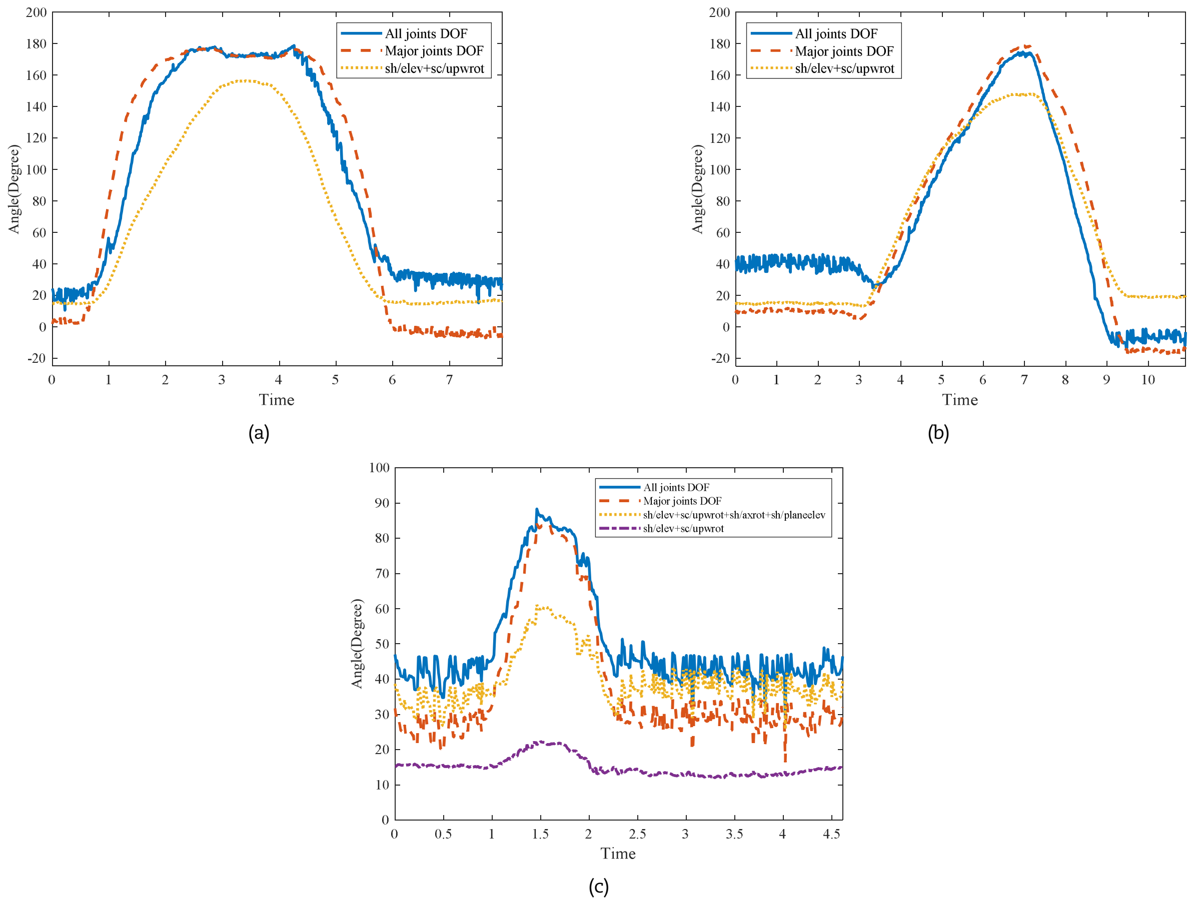

Fig. 8. The summation of the major and all joints DOF in (a) flexion, (b) abduction, (c) shrugging motion.

Table 7. The major joint DOF of the motions.

	Flexion/Extension	Abduction/Adduction	Shrugging
Major DOF	- shoulder elevation - scapula upward rotation - scapula winging - clavicle protraction - shoulder plane elevation - pronation/supination of the radioulnar joint	- shoulder elevation - scapula upward rotation - clavicle protraction - shoulder plane elevation - pronation/supination of the radioulnar joint	- scapula upward rotation - scapula elevation - clavicle elevation - shoulder elevation - shoulder plane elevation axial rotation

Table 8. The Major DOFs, the primary muscles and the correspondent synergy during different motions.

Abduction motion			Flexion motion		
Major DOF	Primary muscles (Literature review)	Correspondent synergy	Major DOF	Dominant muscles (Literature review)	Correspondent synergy
Shoulder abduction Shoulder plane abduction	MD TS SA Infra	Syn3	Shoulder Flexion	AD PM Cb Bic	Syn 3
Shoulder adduction Shoulder plane adduction	PM LatD T-Major Sub	Syn 2	Shoulder Extension	Tric T-major PD	Syn 4
Scapula upward rotation	SA TS	Syn1	Scapula upward rotation	TS SA	Syn 2
Scapula downward rotation	LS Rh PMinor TMajor	Syn4	Shoulder plane abduction	SA MD Infra TS	Syn 1
Shrugging motion					
Major DOF	Dominant muscles (Literature review)	Correspondent synergy	Major DOF	Dominant muscles (Literature review)	Correspondent synergy
Clavicle elevation Scapula elevation	LS TS	Syn2	Shoulder depression Scapula downward rotation	LS PMinor SA	Syn 1

The joints DOF effective in shrugging motion are scapula upward rotation, scapula elevation, clavicle elevation, shoulder elevation, shoulder plane elevation and axial rotation. Figure 8(c) shows the shoulder complex motion of the five major DOF in comparison to the full range of motion. It is concluded from Fig. 8(c) that the only summation of shoulder elevation and scapula upward rotation will not compose the full range motion, therefore, the axial rotation and the plane elevation of the GH joint must be contributed to be approximately close to the full range motion. Table 7 presents the major degrees of freedom (DOF) for different motions. Subsequently, the muscles involved in these major DOF are identified based on previous kinesiological studies. The results are then compared with the dominant muscles identified through muscle synergies. Consequently, the activation times of each muscle group, relative to the corresponding joint DOF, are extracted.

5. Discussion

The aim of this study is to distinguish the dominant muscles in each phase of motion by applying the muscle synergy and inverse kinematic approach in three basic motions. Extracting muscles synergies is the first step in which the dominant muscles were identified due to the relative maximum of the muscle coefficients in each synergy with respect to other muscles. The dominant muscles in each synergy cooperate together as the muscle groups in each phase of motion. The activation time of muscle groups is obtained by comparing the muscle activations diagrams with synergy versus time in each synergy plot. The peaks, increases and decreases in synergies versus time diagrams are considered to determine the activation time of the muscle groups. To realize about the relation between the activation of the muscle groups activation with the phase of motion, the inverse kinematic approach is applied. The aim of applying the inverse kinematic approach is to distinguish the minimum major joints DOF of the musculoskeletal model by computing the joints angles in three basic motions. This process is performed based on two criteria: 1) the most variations of the angles in each DOF, 2) the most impact of each DOF in summation of the angles to compose full range of motion. By extracting the minimum major DOF, the dominant muscles which contribute to move each major DOF are obtained according to the literature. Then, the dominant muscles are compared by the two inverse kinematic and NNMF approaches.

The major DOF in flexion motion are shoulder elevation and scapula upward rotation. The primary muscles of the shoulder elevation in flexion motion are AD, PM, Coracobrachialis (Cb) and Bic [36, 37] that correspond to the synergy 3 of the flexion motion in Fig. 4. The primary muscles of the shoulder elevation of the GH joint in extension motion are triceps (Tric), T-Major and PD [38, 39] that form synergy 4 of the extension motion in Fig. 4. The other major DOF in flexion motion is scapula upward rotation. The primary muscles in scapula upward rotation are TS and the SA [40]. The SA muscle has the role of preserving the scapula against the thorax. These dominant muscles are corresponded with synergy 2 of the flexion motion. These synergies are known as stabilizer synergies.

The major DOF in abduction motion is shoulder elevation. The primary muscles of the shoulder elevation in abduction motion are the MD which is activated for approximately 15 to 90 degree and the TS and the SA which allow the abduction beyond 90 degrees [41, 42]. These dominant muscles are corresponded with the synergy 3 of the motion in Fig. 5. The TS and SA muscles are synergists with the deltoid muscles for the abduction motion and also prevent the undesired downward rotation of the scapula [43]. The dominant muscles of the adduction motion are the PM, LattismusDorsi (LatD) [44]. These muscles are corresponded with the synergy 2 in Fig. 5. The T-Major and rhomboid (Rh) muscles have the cooperation to stabilize the scapula during the humerus adduction [45] . When the scapula is fixed, the T-Major muscle can move the humerus. This is approved in synergy 4 of Fig. 5.

In shrugging motion, the first phase is 0 to 90 degrees and the second phase is 90 to 0 degrees. The major DOF in shrugging motion are clavicle elevation, scapula upward rotation, shoulder plane elevation, shoulder elevation and axial rotation. The major muscles of the clavicle and scapula elevation are levator scapular (LS) and the TS [46], which correspond to synergy 2 in Fig. 6. The other major DOF in shrugging motion is axial rotation. The clavicular head of the PM muscle can produce the medial rotation of the humerus that is correspond to the synergy 2 of the shrugging motion in the first phase (Fig. 6) and also the pectoralis minor muscle has the obligation to depress the shoulder complex that is activated in the synergy 1 of the shrugging motion in the second phase of motion [47, 48]. As the result of Fig. 6 shown, synergy 2 of the shrugging motion is related to the first phase of motion (0 to 80 degrees) and synergy 1 is related to the second phase of motion (80 to 0 degrees). The explanation of the primary muscles, Major DOF and the correspondent synergy is mentioned in table 2. Due to the high conformity between the IK and NNMF approaches, the relationship between muscle group activation and the major DOF involved in each phase of motion was studied. This analysis is valuable in shoulder biomechanics for understanding the reasons behind motion due to muscle cooperation. The results are summarized in Table 8.

Regarding the limitations of this study, it is noted that computing muscle activation can introduce errors compared to experimental measurements. Additionally, measuring all muscle activations is challenging due to crosstalk and the presence of deep muscles. Therefore, an optimization approach is used to estimate all muscle activations involved in upper limb motions. Another limitation is that subjects must perform upper limb motions with electromyography and kinematic markers attached to their skin.

6. Conclusions

In this study, the relation between dominant muscles and the major DOF to perform a specific motion was investigated. For this purpose, the SMM was first verified and the activation of twenty-one muscles was extracted. Muscle synergies were extracted using the NNMF method to identify the dominant muscles in each phase of motion. The IK method was then applied to determine joint angles and identify the major DOF for each motion based on joint angle variations. Dominant muscles in the synergies indicate the cause of motion, while the major DOF show the joint angles involved. Therefore, the dominant muscles contributing to the major DOF were identified through a literature review and compared to those extracted by the NNMF method. The relationship between dominant muscle groups and major DOF in different phases of motion represents the main novelty of this research. Base on the results, the dominant muscles in each phase of motion had high conformity by the IK and NNMF approaches. The aim of this research was to understand the relationship between muscles as actuators and joint kinematics in the shoulder complex. The new findings on the relationship between muscle group activation and major DOF will be valuable for designing rehabilitation exercises that target specific muscles based on the phase of motion, or for developing rehabilitation orthoses tailored to specific muscles.

A limitation of this study is the reliance on computational methods for measuring muscle activations, which can introduce errors compared to experimental measurements. The experiments were conducted on healthy subjects, and only superficial muscle EMG was measured due to existing constraints. Future work will involve investigating muscle cooperation in subjects with neural disorders. Additionally, the similarity and combination of muscle synergies during basic and complex upper limb motions will be explored.

Author Contributions

M. Farrokhnia, S.A. Haghpanah, and E. Ghavanloo planned the scheme, initiated the project, developed the mathematical modeling, and validated the theory. M. Farrokhnia and M.T. Karimi suggested and conducted the experiments, and analyzed the empirical results. The manuscript was written with contributions from all authors. All authors discussed the results, reviewed, and approved the final version of the manuscript.

Acknowledgments

The authors are grateful to Dr. Majlesi for fruitful discussions and advice.

Conflict of Interest

The authors declared no potential conflicts of interest concerning the research, authorship, and publication of this article.

Funding

The authors received no financial support for the research, authorship, and publication of this article.

Data Availability Statements

The datasets generated and/or analyzed during the current study are available from the corresponding author on reasonable request.

Nomenclature

Tminor	Teres minor	PM-Clav	pectoralis major clavicular head
Tmajor	Teres major	PM-Stern	pectoralis major sternal head
Tric	Triceps	AD	Anterior deltoid
TS	superior trapezius	PD	posterior deltoids
TI	inferior trapezius	MD	Middle deltoids
TM	middle trapezius	Infra	Infraspinats
Sub	Subscapularis	Bic	Biceps

Sup	Supraspinatus	LD	lattismus dorsi
Rh	Rhomboid	Cb	coracobrachialis
Pminor	Pectoralis minor	LS	levator scapulae

References

[1] Kian, A., Pizzolato, C., Halaki, M., Ginn, K., Lloyd, D., Reed, D., Ackland, D., Static optimization underestimates antagonist muscle activity at the glenohumeral joint: A musculoskeletal modeling study, *Journal of Biomechanics*, 97, 2019, 109348.
[2] Van der Helm, F.C., A finite element musculoskeletal model of the shoulder mechanism, *Journal of Biomechanics*, 27, 1994, 551-69.
[3] Holzbaur, K.R., Murray, W.M., Delp, S.L., A model of the upper extremity for simulating musculoskeletal surgery and analyzing neuromuscular control, *Annals of Biomedical Engineering*, 33, 2005, 829-840.
[4] Blache, Y. and Begon, M., Influence of shoulder kinematic estimate on joint and muscle mechanics predicted by musculoskeletal model, *IEEE Transactions on Biomedical Engineering*, 65, 2017, 715-722.
[5] Saul, K.R., Hu, X., Goehler, C.M., Vidt, M.E., Daly, M., Velisar, A., Murray, W.M., Benchmarking of dynamic simulation predictions in two software platforms using an upper limb musculoskeletal model, *Computer Methods in Biomechanics and Biomedical Engineering*, 18, 2015, 1445-1458.
[6] Charlton, I.W. and Johnson, G.R., A model for the prediction of the forces at the glenohumeral joint, *Proceedings of the Institution of Mechanical Engineers, Part H: Journal of Engineering in Medicine*, 220, 2006, 801-812.
[7] Fayad, F., Roby-Brami, A., Yazbeck, C., Hanneton, S., Lefevre-Colau, M.M., Gautheron, V., Poiraudeau, S., Revel, M., Three-dimensional scapular kinematics and scapulohumeral rhythm in patients with glenohumeral osteoarthritis or frozen shoulder, *Journal of Biomechanics*, 41, 2008, 326-332.
[8] Bolsterlee, B., Veeger, D.H., Chadwick, E.K., Clinical applications of musculoskeletal modelling for the shoulder and upper limb, *Medical & Biological Engineering & Computing*, 51, 2013, 953-963.
[9] Seth, A., Matias, R., Veloso, A.P., Delp, S.L., A biomechanical model of the scapulothoracic joint to accurately capture scapular kinematics during shoulder movements, *PLOS ONE*, 11, 2016, e0141028.
[10] Odle, B., Reinbolt, J., Forrest, G., Dyson-Hudson, T., Construction and evaluation of a model for wheelchair propulsion in an individual with tetraplegia, *Medical & Biological Engineering & Computing*, 57, 2019, 519-532.
[11] Seth, A., Dong, M., Matias, R., Delp, S., Muscle contributions to upper-extremity movement and work from a musculoskeletal model of the human shoulder, *Frontiers in Neurorobotics*, 13, 2019, 90.
[12] Li, G., Kaufman, K.R., Chao, E.Y.S., Rubash, H.E., Prediction of antagonistic muscle forces using inverse dynamic optimization during flexion/extension of the knee, *Journal of Biomechanical Engineering*, 121, 1999, 316-322.
[13] Brookham, R.L., Middlebrook, E.E., Grewal, T.J., Dickerson, C.R., The utility of an empirically derived co-activation ratio for muscle force prediction through optimization, *Journal of Biomechanics*, 44, 2011, 1582-1587.
[14] Arnold, E.M., Ward, S.R., Lieber, R.L., Delp, S.L., A model of the lower limb for analysis of human movement, *Annals of Biomedical Engineering*, 38, 2010, 269-279.
[15] Terrier, A., Aeberhard, M., Michellod, Y., Mullhaupt, P., Gillet, D., Farron, A., Pioletti, D.P., A musculoskeletal shoulder model based on pseudo-inverse and null-space optimization, *Medical Engineering & Physics*, 32, 2010, 1050-1056.
[16] Gagnon, D., Arjmand, N., Plamondon, A., Shirazi-Adl, A., Larivière, C., An improved multi-joint EMG-assisted optimization approach to estimate joint and muscle forces in a musculoskeletal model of the lumbar spine, *Journal of Biomechanics*, 44, 2011, 1521-1529.
[17] Forster, E., Simon, U., Augat, P., Claes, L., Extension of a state-of-the-art optimization criterion to predict co-contraction, *Journal of Biomechanics*, 37, 2004, 577-581.
[18] Engelhardt, C., Malfroy Camine, V., Ingram, D., Müllhaupt, P., Farron, A., Pioletti, D., Terrier, A., Comparison of an EMG-based and a stress-based method to predict shoulder muscle forces, *Computer Methods in Biomechanics and Biomedical Engineering*, 18, 2015, 1272-1279.
[19] Ding, Z., Azmi, N.L., Bull, A.M., Validation and use of a musculoskeletal gait model to study the role of functional electrical stimulation, *IEEE Transactions on Biomedical Engineering*, 66, 2018, 892-897.
[20] Sarshari, E., Mancuso, M., Terrier, A., Farron, A., Mullhaupt, P., Pioletti, D., Muscle co-contraction in an upper limb musculoskeletal model: EMG-assisted vs. standard load-sharing, *Computer Methods in Biomechanics and Biomedical Engineering*, 24, 2021, 137-150.
[21] Lambert-Shirzad, N., *Upper-body motion coordination after stroke: insights from kinematic and muscle synergies*, Doctoral Dissertation, University of British Columbia, 2017.
[22] Guigon, E., Models and architectures for motor control: Simple or complex, *Motor Control*, 20, 2011, 478-502.
[23] Sartori, M., Lloyd, D.G., Farina, D., Neural data-driven musculoskeletal modeling for personalized neurorehabilitation technologies, *IEEE Transactions on Biomedical Engineering*, 63, 2016, 879-893.
[24] Turvey, M.T., Coordination, *American Psychologist*, 45, 1990, 938.
[25] Mazumder, O., Rai, A., Sinha, A., Muscle synergy control during hand reach task on varying shoulder configuration, *Proceedings of the IEEE Engineering in Medicine & Biology Society Annual International Conference*, 42, 2020, 4839-4843.
[26] Esmaeili, J., Maleki, A., Comparison of muscle synergies extracted from both legs during cycling at different mechanical conditions, *Australasian Physical & Engineering Sciences in Medicine*, 42, 2019, 827-838.
[27] Baniasad, M., Farahmand, F., Arazpour, M., Zohoor, H., Coordinated activities of trunk and upper extremity muscles during walker-assisted paraplegic gait: A synergy study, *Human Movement Science*, 62, 2018, 184-193.
[28] Wu, G., Van der Helm, F.C., Veeger, H.D., Makhsous, M., Van Roy, P., Anglin, C., Nagels, J., Karduna, A.R., McQuade, K., Wang, X., Werner, F.W., ISB recommendation on definitions of joint coordinate systems of various joints for the reporting of human joint motion—Part II: Shoulder, elbow, wrist and hand, *Journal of Biomechanics*, 38, 2005, 981-992.
[29] Seth, A., Sherman, M., Eastman, P., Delp, S., Minimal formulation of joint motion for biomechanisms, *Nonlinear Dynamics*, 62, 2010, 291-303.
[30] Thelen, D.G., Anderson, F.C., Using computed muscle control to generate forward dynamic simulations of human walking from experimental data, *Journal of Biomechanics*, 39, 2006, 1107-1115.
[31] Porsa, S., Lin, Y.C., Pandy, M.G., Direct methods for predicting movement biomechanics based upon optimal control theory with implementation in OpenSim, *Annals of Biomedical Engineering*, 44, 2016, 2542-2557.
[32] Lambert-Shirzad, N., Van Der Loos, H.M., On identifying kinematic and muscle synergies: a comparison of matrix factorization methods using experimental data from the healthy population, *Journal of Neurophysiology*, 117, 2017, 290-302.
[33] Saito, A., Tomita, A., Ando, R., Watanabe, K., Akima, H., Muscle synergies are consistent across level and uphill treadmill running, *Scientific Reports*, 8, 2018, 5979.
[34] Zhao, Y., Li, Z., Zhang, Z., Qian, K., Xie, S., An EMG-driven musculoskeletal model for estimation of wrist kinematics using mirrored bilateral movement, *Biomedical Signal Processing and Control*, 81, 2023, 104480.
[35] Wang, S., Hase, K., Funato, T., Computational prediction of muscle synergy using a finite element framework for a musculoskeletal model on lower limb, *Frontiers in Bioengineering and Biotechnology*, 11, 2023, 1130219.
[36] Soames, R.W., *Anatomy and Human Movement: Structure and Function*, Elsevier Health Sciences, 2023.
[37] Cael, C., *Functional Anatomy: Musculoskeletal Anatomy, Kinesiology, and Palpation for Manual Therapists*, Jones & Bartlett Learning, 2022.
[38] Levangie, P.K., Norkin, C.C., *Joint Structure and Function: A Comprehensive Analysis*, FA Davis, 2011.
[39] Konrad, G.G., Jolly, J.T., Labriola, J.E., McMahon, P.J., Debski, R.E., Thoracohumeral muscle activity alters glenohumeral joint biomechanics during active abduction, *Journal of Orthopaedic Research*, 24, 2006, 748-756.
[40] Likens, A.D., Stergiou, N., *Basic Biomechanics*, Biomechanics and Gait Analysis, 2020, 16.
[41] Labriola, J.E., Lee, T.Q., Debski, R.E., McMahon, P.J., Stability and instability of the glenohumeral joint: the role of shoulder muscles, *Journal of Shoulder and Elbow Surgery*, 14, 2005, S32-S38.
[42] Walker, P.S., Poppen, N.K., Biomechanics of the shoulder joint during abduction in the plane of the scapula, *Bulletin of the Hospital for Joint Diseases*, 38, 1977, 107-111.
[43] Ludewig, P.M., Phadke, V., Braman, J.P., Hassett, D.R., Cieminski, C.J., LaPrade, R.F., Motion of the shoulder complex during multiplanar humeral

elevation, *Journal of Bone and Joint Surgery*, 91, 2009, 378-389.
[44] Poppen, N.K., Walker, P.S., Forces at the glenohumeral joint in abduction, *Clinical Orthopaedics and Related Research*, 135, 1978, 165-170.
[45] FAPTA, D.A.N.P.P., Kinesiology of the Musculoskeletal System: Foundations for Rehabilitation, 2010.
[46] Conway, A.M., Movements at the sternoclavicular and acromioclavicular joints, *Physical Therapy*, 41, 1961, 421-432.
[47] Shizukuda, K., Hata, Y., Ishigaki, N., Takahashi, T., Tajima, Y., Mimura, R., Maeda, S., Impact of Shoulder Shrugging Motion on Muscles Surrounding the Shoulder Joint during Forward Elevation of the Upper Limb, *Journal of the Japanese Association of Rural Medicine*, 65, 2017, 940-945.
[48] Castelein, B., Cools, A., Parlevliet, T., Cagnie, B., Modifying the shoulder joint position during shrugging and retraction exercises alters the activation of the medial scapular muscles, *Manual Therapy*, 21, 2016, 250-255.

ORCID iD

Morteza Farrokhnia https://orcid.org/0000-0002-6616-6551
Seyyed Arash Haghpanah https://orcid.org/0000-0002-3121-0161
Esmaeal Ghavanloo https://orcid.org/0000-0002-2376-3751
Mohammad Taghi Karimi https://orcid.org/0000-0001-6162-8131

How to cite this article: Farrokhnia M., Haghpanah S.A., Ghavanloo E., Karimi M.T. Relation of Muscles Coordination to the Major Degrees of Freedom in Three Upper Limb Motions, *J. Appl. Comput. Mech.*, 11(4), 2025, 961-974. https://doi.org/10.22055/jacm.2024.47305.4692